



Sap flux-scaled transpiration and stomatal conductance response to soil and atmospheric drought in a semi-arid sagebrush ecosystem

Kusum J. Naithani*, Brent E. Ewers, Elise Pendall

Department of Botany, University of Wyoming, Laramie, WY 82071, USA
 Program in Ecology, University of Wyoming, Laramie, WY 82071, USA

ARTICLE INFO

Article history:

Received 10 August 2011

Received in revised form 17 March 2012

Accepted 6 July 2012

Available online 16 July 2012

This manuscript was handled by Laurent Charlet, Editor-in-Chief, with the assistance of Sheng Yue, Associate Editor

Keywords:

Drought
 Leaf transpiration
 Plant hydraulic model
 Sap flux
 Shrubs
 Stomatal conductance

SUMMARY

Arid and semi-arid ecosystems represent a dynamic but poorly understood component of global carbon, water, and energy cycles. We studied a semi-arid mountain big sagebrush (*Artemisia tridentata* var. *vas-eyana*; hereafter, "sagebrush") dominated ecosystem to quantify the (1) relative control of surface (0–15 cm) versus deep (15–45 cm) soil moisture on leaf transpiration (E_L) and stomatal conductance (g_S); (2) response of E_L and g_S to light and soil and atmospheric drought; and (3) physiological mechanisms underlying these responses. The physiological mechanisms were tested using a simple plant hydraulic model for g_S based on homeostatic regulation of minimum leaf water potential (Ψ_{Lmin}) that was originally developed for trees. Our results showed that a combination of atmospheric and surface soil drought controlled E_L , whereas g_S was mainly driven by atmospheric drought. Sagebrush displayed greater reference conductance [$g_S @ 1$ kPa vapor pressure deficit (D), g_{SR}] and greater sensitivity ($-m$) of g_S to D than mesic trees, reflecting the high average light intensity within the shrub canopy. The slope of $-m/g_{SR}$ was similar to mesic trees (~ 0.6), indicating an isohydric regulation of Ψ_{Lmin} , but different than previously published values for semi-arid shrubs (~ 0.4). Isohydric behavior of sagebrush indicates that well-known forest ecosystem models with greater g_{SR} and $-m$ can be used for modeling water, energy and carbon cycles from sagebrush and similar ecosystems.

© 2012 Elsevier B.V. All rights reserved.

1. Introduction

About 40% of the Earth's terrestrial surface is covered by arid and semi-arid ecosystems which are expanding globally (Schlesinger, 1997; Reynolds, 2000). Global and regional climate models predict a change in plant productivity in response to changing temperature and precipitation patterns, especially in arid and semi-arid ecosystems (Easterling et al., 2000; NAST, 2001; Bates et al., 2008), which are subjected to strong seasonal cycles of rainfall and extended drought (Smith and Allen, 1996; Sivakumar et al., 2005) and may not be predictable from more intensively studied mesic ecosystems (Ogle and Reynolds, 2002, 2004). Understanding physiological responses of arid and semi-arid vegetation to soil and atmospheric drought and the underlying mechanisms is critical for accurate prediction of long term ecosystem carbon, water and, energy fluxes and will provide a more mechanistic picture of plant response to drought.

Stomatal conductance (g_S) couples photosynthesis and transpiration (Cowan and Farquhar, 1977), which makes it a key

* Corresponding author. Present address: 302 Walker Building, The Pennsylvania State University, University Park, PA 16802, USA. Tel.: +1 814 865 7432; fax: +1 814 863 7943.

E-mail address: naithani@psu.edu (K.J. Naithani).

parameter in climate models for quantifying biosphere–atmosphere interactions (Sellers et al., 1997; Lai et al., 2002; Baldocchi et al., 2002; Schäfer et al., 2003). g_S can be estimated at leaf scales by using instantaneous gas exchange measurements (Jarvis, 1995) and from branch to ecosystem scales by continuous sap flux and eddy covariance techniques (Köstner et al., 1992). Sap flux provides species-specific transpiration rates (Cermák et al., 1995; Ewers et al., 2002; Baldocchi, 2005) and can be used for continuous estimation of leaf and canopy g_S and its response to environmental variables at sub-daily time scales (Köstner et al., 1992; Phillips and Oren, 1998; Ewers et al., 2007). However, prior studies on response of sap flux-scaled transpiration and g_S are heavily biased from forest ecosystems (see Mackay et al., 2010 for a comprehensive list) with few sap flux field studies in arid and semi-arid ecosystems (e.g., Oren et al., 1999; Pataki et al., 2000; Dawson et al., 2007; Qu et al., 2007; Lei et al., 2010). This paucity of sap flux field data for arid and semi-arid shrub ecosystems needs to be addressed to improve current and future prediction of long term ecosystem carbon, water, and energy fluxes.

The current understanding of transpiration suggests that leaf water potential (Ψ_L) plays an important role in regulation of transpiration which in turn is dependent on whole plant water status (Meinzer and Grantz, 1991; Mott and Parkhurst, 1991; Saliendra et al., 1995; Cochard et al., 1996; Nardini and Salleo, 2000; Salleo

Nomenclature

Abbreviation

D	leaf to air vapor pressure deficit (kPa)
D_{max}	maximum D
DI	drought index
E_L	leaf transpiration rate ($\text{mmol m}^{-2} \text{s}^{-1}$)
E_R	root sap flux (mmol s^{-1})
E_{Rmax}	maximum root sap flux (mmol s^{-1})
g_S	stomatal conductance of water vapor ($\text{mmol m}^{-2} \text{s}^{-1}$)
g_{Smax}	theoretical maximum stomatal conductance ($\text{mmol m}^{-2} \text{s}^{-1}$)
g_{SR}	reference stomatal conductance ($\text{mmol m}^{-2} \text{s}^{-1}$)
K_G	conductance coefficient ($\text{kPa m}^3 \text{kg}^{-1}$)
K_L	leaf-specific whole-plant hydraulic conductance ($\text{kg m}^{-2} \text{s}^{-1} \text{MPa}^{-1}$)

L	leaf area index ($\text{m}^2 \text{m}^{-2}$)
m	stomatal sensitivity to D ($\text{mmol m}^{-2} \text{s}^{-1} \text{kPa}^{-1}$)
Q	photosynthetically active photon flux density ($\mu\text{mol m}^{-2} \text{s}^{-1}$)
T_{Air}	air temperature ($^{\circ}\text{C}$).

Greek letters

θ_V	volumetric soil water content ($\text{m}^3 \text{m}^{-3}$)
Ψ_L	leaf water potential (MPa)
Ψ_{Lmin}	minimum leaf water potential (MPa)
Ψ_S	soil water potential (MPa)
Ψ_g	gravitational water potential (MPa)

et al., 2000; Mott and Franks, 2001; Franks, 2004; Franks et al., 2007; Johnson et al., 2009). To understand the mechanisms involved in stomatal behavior, it is important to analyze the response of g_S to vapor pressure deficit (D) (Monteith, 1995) by studying the hydraulic regulation of transpiration and Ψ_L (Oren et al., 1999), which avoids catastrophic xylem cavitation (Tyree and Sperry, 1989; Sperry et al., 1998). In isohydric plants (Tardieu and Simonneau, 1998; Franks et al., 2007), the homeostatic regulation of minimum Ψ_L (Ψ_{Lmin}) is necessary to maintain equilibrium between maximum water supply and optimal photosynthesis (Katul et al., 2003; Katul et al., 2009). Darcy's Law describes the water side of this equilibrium at steady state (Whitehead and Jarvis, 1981; Whitehead et al., 1984; Sperry, 1995) as:

$$g_S \frac{L}{D} (\Psi_S - \Psi_L - \Psi_g) \quad (1)$$

where g_S is stomatal conductance for water vapor, K_L is leaf-specific whole-plant hydraulic conductance, Ψ_S is soil water potential, and Ψ_g is gravitational potential. As soil dries out, K_L declines with declining Ψ_S and this decline in K_L requires further decrease in Ψ_L to sustain increasing transpiration (Sperry et al., 1998). Hydraulic failure occurs when transpiration exceeds the water supply, which drives K_L to zero and is referred to as run-away cavitation (Tyree and Sperry, 1989).

Because the signaling mechanisms which integrate leaf and root controls on g_S are still unknown (Franks et al., 2007; Fujii et al., 2009; Pandey et al., 2010), g_S responses to environmental drivers are still predicted semi-mechanistically with models, such as the Ball–Woodrow–Berry (1987) or the Jarvis (1976) model consisting of multiplicative nonlinear functions of environmental variables:

$$g_S = g_{Smax} f_1(D) f_2(Q) f_3(T_{Air}) f_4(\Psi_L) \quad (2)$$

where g_{Smax} is the theoretical maximum g_S observed in fully developed leaves before senescence, in plants growing under optimal water, nutrient, and climatic conditions (Körner, 1994), Q is photosynthetically active photon flux density, and T_{Air} is ambient temperature. Oren et al. (1999) used a logarithmic relationship to put a mechanism in the $f_1(D)$ portion of Eq. (2):

$$g_S = g_{SR} - m \ln D \quad (3)$$

where g_{SR} is g_S at 1 kPa D and m is the stomatal sensitivity to $\ln D$ or the slope of stomatal response to logarithmic D ($m = \frac{\partial g_S}{\partial \ln D}$). This work and others (Oren et al., 1999, 2001; Ewers et al., 2001b; Gunderson et al., 2002; Addington et al., 2004) showed that $-m \sim 0.6 g_{SR}$ for a wide range of environmental conditions in mesic tree species. The 0.6 proportionality can be explained by the homeostatic regulation

of Ψ_{Lmin} to prevent damagingly low xylem water potential which leads to cavitation (Eq. (1)). Deviations from 0.6 proportionality can occur when: (1) a species can adjust Ψ_{Lmin} to decline with increasing D (anisohydric); (2) a species experiences a wide range of D ; and (3) boundary layer conductance to g_S ratio is low (Oren et al., 1999). The first two conditions arise due to different drought response mechanisms of species that tolerate high water column tensions, such as arid and semi-arid shrub species (Oren et al., 1999; Ogle and Reynolds, 2002: $-m/g_{SR} \sim 0.46$), which lowers the 0.6 proportionality; the third condition gives higher proportionality than 0.6 (Oren et al., 1999).

Mencuccini's (2003) synthesis of the plant hydraulic literature showed that arid/semi-arid shrubs have the highest K_L and g_S of all the plant functional types surveyed. This synthesis coupled with results from arid/semi-arid shrubs showing a proportion between $-m$ and g_{SR} as low as 0.4 led us to test whether the semi-arid shrub, mountain big sagebrush (*Artemisia tridentata* var. *vaseyana* (Rydb.) Beetle) is similar to other arid/semi-arid shrubs. Sagebrush-steppe is a dominant vegetation type of Intermountain west and covers approximately 630,000 km² of North America (West, 1983). Sagebrush is known for surviving in water limited conditions by physiological adaptations. It displays hydraulic redistribution, the movement of water [upwards (e.g., Richards and Caldwell, 1987), downwards (e.g., Brooks et al., 2006), and laterally (Hultine et al., 2003)] across a gradient of Ψ_S from high Ψ_S (wet soil) to low or more negative Ψ_S (dry soil) (Richards and Caldwell, 1987; Caldwell and Richards, 1989; Caldwell et al., 1998), and uses deep taproots as well as shallow, diffuse roots (Sturges, 1977). In a previous study of sagebrush ecosystem by Kwon et al. (2008), the net ecosystem exchange (NEE) showed greater dependence on deep soil moisture (15–45 cm) than surface soil (4 cm). We tested the hypothesis proposed by Kwon et al. (2008) for NEE to assess if E_L and g_S also depend on deep soil moisture. Previous studies on trees (Matsumoto et al., 2005) and crop ecosystems (Irmak and Mutiibwa, 2010) reported that variability in g_S is explained mostly by Q , T_{Air} and relative humidity (RH) and θ_V explained the least variation. We tested this hypothesis by quantifying the relative control of Q and soil and atmospheric drought on E_L and g_S under field conditions in a sagebrush ecosystem. In addition, we tested a simple plant-hydraulic model (Oren et al., 1999), as described above, to understand underlying mechanisms of hydraulic control and asked the following questions: (1) are E_L and g_S controlled more by surface (0–15 cm) or deep (15–45 cm) soil moisture?; (2) what is the relative control of Q and soil and atmospheric drought on E_L and g_S ?; and (3) is mountain big sagebrush similar to other arid/semi-arid shrubs and different than mesic trees in terms of reference conductance (g_{SR}) and the ratio ($-m/g_{SR}$)?

2. Materials and methods

2.1. Study area

This study was conducted during the growing season (May–October) of 2005 in a semi-arid mountain big sagebrush (*A. tridentata* var. *vaseyana*) ecosystem located at ~2270 m elevation (N41°21'23": W107°23'33") in the northwest of the Sierra Madre Mountain Range, Wyoming, USA. The study area was dominated by mountain big sagebrush with scattered grasses, such as western wheatgrass (*Pascopyrum smithii*), needle and thread (*Hesperostipa comata*), Idaho fescue (*Festuca idahoensis*), and forbs, such as silvery lupine (*Lupinus argenteus*). The canopy height was about 1 m with $1.2 \text{ m}^2 \text{ m}^{-2}$ leaf area index (L) and ~39% vegetation cover (Kwon et al., 2008). The site climate was marked with long, cold winters (~7 month snow presence) and warm, dry summers with 259–341 mm annual precipitation and 6.2–7.2 °C annual temperature (Ewers and Pendall, 2008). Surface soil texture was sandy clay loam and deep (below 20 cm) soil texture was clay loam (Cleary et al., 2010).

2.2. Meteorological measurements

T_{Air} and relative humidity (RH) were measured by a T_{Air}/RH probe (Model HMP45C, Vaisala, Helsinki, Finland) and Q was measured by a quantum sensor (Model Li-190SZ, Li-COR) at 2.5 m height. D was calculated from RH and T_{Air} measurements using Goff and Gratch (1946) equation. A tipping-bucket rain gauge (Model TE525MM, Texas Electronics, Texas, USA) was used to measure precipitation (mm) and soil moisture probes (Model CS616, Campbell Scientific) were used for continuous measurements of volumetric soil water content (θ_V) at two soil depths (0–15 cm and 15–45 cm). Dewpoint potentiometer (Model WP4-T, Decagon Devices, Pullman, WA, USA) was used to generate soil moisture release curves from soil samples collected at abovementioned soil depths. The relationship between θ_V and Ψ_S was used to calculate continuous Ψ_S .

2.3. Sap flux measurements

Continuous sap flux measurements were recorded using the Sap Flow Meter-T4.1 (EMS Brno, Czech Republic) (e.g., Kučera et al., 1977; Cenciala et al., 1994; Cermák et al., 1995). The Sap Flow Meter consists of a datalogger and 12 independent units for supplying electric power to heat the thermocouples at the measuring points to maintain constant temperature difference (4 °C) between heated and non-heated part of the gauge. This system works on a constant heating approach which is also known as the tissue heat balance method (Čermák et al., 1973; Kučera, 1977). The tissue heat balance approach provides truly continuous measurements unlike heat pulse method which requires time to reach at steady state after switching off heating (Köstner et al., 1998). The following equation describes the heat balance of tissues through which the sap flow passes:

$$P = RdTcw + dTz \quad (4)$$

where sap flow rate (R ; kg s^{-1}) is calculated based on the temperature difference (dT) and the heat input power (P ; W), at the measuring point. cw and z represent the specific heat of water (cw ; $\text{J kg}^{-1} \text{ }^\circ\text{C}^{-1}$) and coefficient of heat loss (z ; $\text{W }^\circ\text{C}^{-1}$) from the measuring point (Kučera et al., 1977; Smith and Allen, 1996). The magnitude of heat loss can be estimated from the data recorded under condition of actual flow approximating zero, i.e., after a long-term rain or on nights when D is low. Sensors were shielded with mylar to avoid thermal gradients from direct radiation. These sensors do

not require additional scaling measurements, because they measure the entire sap flux of the stem for diameters between 12 mm and 18 mm. Eight stem sap flux sensors were installed on May 25, 2005 and two of those shrubs were selected to install bidirectional root sensors (two sensors on each root) (Fig. S1 in Supplementary data) on July 8, 2005. Shrubs were selected to capture the variability of plant size (small, medium and large) and soil microhabitat. The range of spatial autocorrelation for shrub cover was 1.3 m (± 0.2 m) (Ewers and Pendall, 2008), so the distance between two neighboring shrubs was kept >2 m to obtain independent replications of sap flux. The root was at an angle ($\sim 45^\circ$) and sap flux sensors were installed at ~ 20 cm depth. The sensor with heater facing the shrub to measure the upwards flow is referred as Upwards Sap flux or "USF" and the sensor with heater in the opposite direction to measure water moving away from shrub is referred as Downwards Sap flux or "DSF" sensor (Fig. S1 in Supplementary data). Sensors were removed on October 10, 2005 and branches were cut and brought back to the laboratory for leaf area measurements. Leaves were removed from branches and scanned for one sided leaf area estimation. Image-J software (Abramoff et al., 2004, available at <http://rsb.info.nih.gov/ij>) was used to calculate leaf area from scanned images. Three stem and two root sensors malfunctioned, so remaining five stem sensors and two root sensors were used for data analyses.

Days with missing data were discarded and only non-rainy days with minimum temperature >0 °C were included in the analyses of stem sap flux data to avoid false signals when sap flux sensors were wet or frozen. Root sap flux data were analyzed for all available days. Daily daytime and nighttime averages of sap flux and meteorological data were calculated using Q as a filter to assign day ($\geq 10 \mu\text{mol m}^{-2} \text{ s}^{-1}$) and night ($<10 \mu\text{mol m}^{-2} \text{ s}^{-1}$). The upwards sap flux (USF) from root sensor was compared with the stem sap flux to check their relationship. Both root and stem sap flux sensors were normalized by the maximum observed sap flux value during July 8–August 24 for the respective sensors and an average of five stem sap flux sensors was compared with one root sap flux sensor.

2.4. Calculations of E_L and g_S

Sap flux was divided by the leaf area of the branch to calculate branch transpiration per unit leaf area (E_L ; $\text{kg m}^{-2} \text{ s}^{-1}$). g_S was calculated from E_L and D using a simplified inversion of Penman–Monteith model (Monteith and Unsworth, 1990)

$$g_S = \frac{K_C(T_{\text{Air}}E_L)}{D} \quad (5)$$

where g_S is the stomatal conductance (m s^{-1}) to water vapor; K_C is conductance coefficient as a function of temperature ($115.8 + 0.4236T_{\text{Air}}$; $\text{kPa m}^3 \text{ kg}^{-1}$) which accounts for temperature effects on the psychrometric constant, latent heat of vaporization, specific heat of air at constant pressure and air density; and T_{Air} is bulk air temperature (°C) used in calculation of K_C (Phillips and Oren, 1998). g_S was converted from m s^{-1} to $\text{mmol m}^{-2} \text{ s}^{-1}$ using atmospheric pressure of the site (78 kPa) and simultaneous temperature measurements (Percy et al., 1989). The simplified inversion of Penman–Monteith assumes large boundary layer conductance, no vertical gradient of D and negligible water storage above the sensor (Ewers and Oren, 2000). The study area conditions matched these assumptions being windy (large boundary layer conductance) and having an open (canopy cover ~39%) and short (canopy height ~1 m) canopy. Daytime ($Q \geq 10 \mu\text{mol m}^{-2} \text{ s}^{-1}$) data were used for calculation of g_S at $D > 0.6$ to minimize relative errors ($<10\%$) (Ewers and Oren, 2000).

2.5. Data and statistical analyses

Two approaches were used to analyze the effects of multiple parameters on g_S and E_L . The first approach analyzed the response

of half hourly (root sap flux, E_R) and daily (stem sap flux, E_L) means (day and night separately) of transpiration and g_S to half hourly and daily means of Q and soil and atmospheric drought respectively. E_R was normalized by the observed maximum daytime root sap flux value (E_{Rmax}) during the growing season (e.g., Dawson et al., 2007) and reported as:

$$E_R[i] = \left(\frac{E_R[i]}{E_{Rmax}} \right) * 100 \quad (6)$$

where $E_R[i]$ is the half hourly mean of root sap flux for a given point in time $[i]$. Soil (at both soil depths) and atmospheric drought were calculated using a similar approach from θ_V (at 0–15 and 15–45 cm depth) and D data that were normalized by the maximum respective values across the growing season. Soil and atmospheric drought were calculated as:

$$\text{Soil Drought}[i] = \left(1 - \frac{\theta_V[i]}{\theta_{Vmax}} \right) * 100 \quad (7)$$

where $\theta_V[i]$ is the half hourly mean of the volumetric soil water content ($\text{m}^3 \text{m}^{-3}$) of a given point $[i]$ in time and θ_{Vmax} is the maximum observed θ_V during the growing season.

$$\text{Atmospheric Drought}[i] = \left(1 - \frac{D[i]}{D_{max}} \right) * 100 \quad (8)$$

where $D[i]$ is the half hourly mean of D at a given point $[i]$ in time and D_{max} is the maximum observed D during the growing season. Drought index (DI) was calculated by averaging the soil and atmospheric droughts:

$$DI[i] = \left(\frac{\text{Soil Drought}[i] + \text{Atmospheric Drought}[i]}{2} \right) \quad (9)$$

The daily values were calculated by averaging half hourly values for day and night hours.

The second approach reduced data to parameters explaining the relationship between g_S and D by performing boundary line analysis under different Q , T_{Air} , and θ_V conditions (Chambers et al., 1985; Pezeshki and Hinckley, 1988; Schäfer et al., 2000; Ewers et al., 2001a). The boundary line analysis was performed by: (1) partitioning data into seven bins of the g_S response to D by keeping equal number of points within each bin; (2) calculating the mean (μ) and standard deviation (σ) of g_S within each D bin; (3) removing outliers ($P < 0.05$ Dixon's test; Sokal and Rohlf, 1995); (4) selecting data more than the " $\mu + \sigma$ " of g_S (Schäfer et al., 2000; Ewers et al., 2001a) to obtain boundary line data. The boundary line represents the highest (optimum physiological) g_S response under measured conditions in a plant or population (Martin et al., 1997). The binned variables (D and $g_S > \mu + \sigma$) were regressed to obtain the g_S response parameters (slope (m) and intercept (g_{SR}) for Eq. (3). Mackay et al. (2003) showed that this boundary line approach provides the same interpretation of Eq. (3) as a full process model of g_S . We also tested the robustness of boundary line analysis under different bin and sample sizes. R statistical software (R Development Core Team, 2010) was used to perform all statistical analyses and SigmaPlot (Systat Software Inc.) was used for preparing graphs.

3. Results

3.1. Are E_L and g_S controlled more by surface (0–15 cm) or deep (15–45 cm) soil moisture?

A general decline in θ_V and Ψ_S was observed in both soil layers during the growing season (Fig. 1a). However, the surface soil (0–15 cm) showed greater range of θ_V and Ψ_S . The change in Ψ_S was greater in surface soil than deep soil despite similar absolute

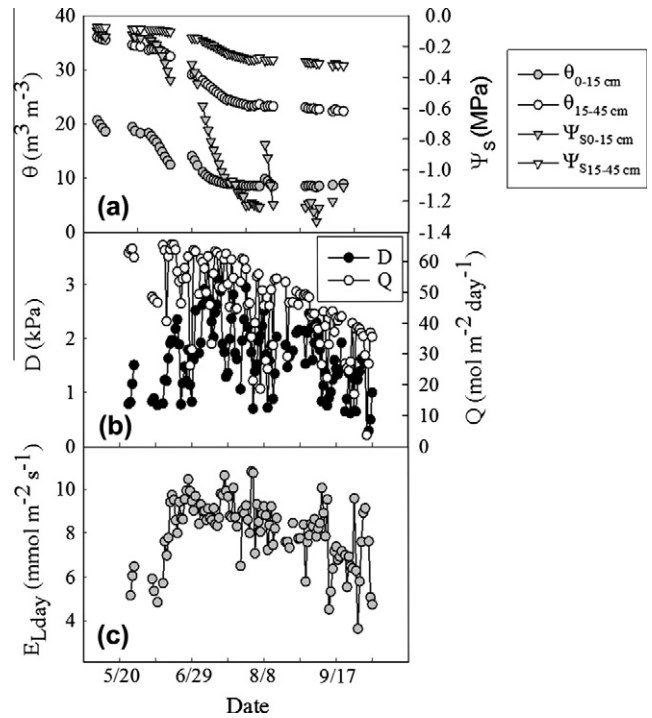


Fig. 1. Seasonal trends of environmental variables and transpiration presented as daily: (a) mean volumetric soil water content (θ_V) and soil water potential (Ψ_S) at 0–15 and 15–45 cm soil depths; (b) sum of photosynthetic photon flux density (Q), mean vapor pressure deficit (D); and (c) mean leaf transpiration (E_L) during the growing season. Daily values were calculated from daytime ($Q \geq 10 \mu\text{mol m}^{-2} \text{s}^{-1}$) data.

changes in the θ_V (Fig. 1a) due to different soil texture [sandy clay loam in the surface and clay loam below 20 cm (Cleary et al., 2010)]. There were noticeable seasonal trends in Q , D , and E_L (Fig. 1b and c). The daily average D and sum of Q displayed similar seasonal declining trend during the growing season (Fig. 1b). The mean daily daytime E_L was low ($\sim 5 \text{ mmol m}^{-2} \text{s}^{-1}$) at the beginning of the growing season (late May) and reached the maximum value ($\sim 11 \text{ mmol m}^{-2} \text{s}^{-1}$) in late June–early July with a declining E_L after early August, which continued until September (Fig. 1c).

Daily daytime ($Q \geq 10 \mu\text{mol m}^{-2} \text{s}^{-1}$) data were used to quantify the effect of soil drought on E_L and g_S at both soil depths. Surface soil drought explained greater ($R^2 = 0.61$) variability in transpiration than deeper soil ($R^2 = 0.47$) (Table S1 in Supplementary data). In addition, g_S showed a weak ($R^2 = 0.18$) exponential decline with surface soil and no relationship with deep soil drought (Table S1 in Supplementary data). Subsequent analyses were done using surface soil (0–15 cm) moisture to see the effect of soil drought on E_L and g_S .

3.2. What is the relative control of Q and soil and atmospheric drought on E_L and g_S ?

Stem sap flux sensors showed diel E_L closely following D and displayed minimum E_L during early morning ($\sim 2 \text{ mmol m}^{-2} \text{s}^{-1}$) and night ($1\text{--}5 \text{ mmol m}^{-2} \text{s}^{-1}$) and maximum ($10\text{--}22 \text{ mmol m}^{-2} \text{s}^{-1}$) E_L during mid-day (Fig. 2a and b). Nighttime and early morning D rarely reached zero (e.g. Fig. 2b) which was reflected in similar E_L trends and values greater than zero at nighttime. The USF sensor showed diel trends similar to D and the DSF sensor showed negative sap flow (downward movement of water) only after a rainfall event (Fig. 3a and b). The corresponding Ψ_S showed wetting of surface soil (greater Ψ_S at 0–15 cm) during rain event and gradual drying (lower Ψ_S at 0–15 cm) after the rain event (Fig. 3a and c). The

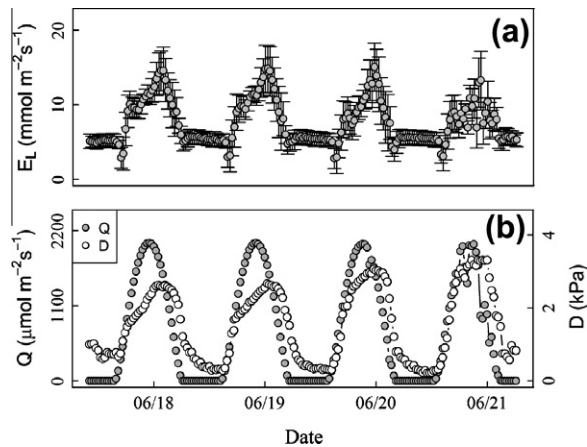


Fig. 2. Representative diel patterns of: (a) leaf transpiration (E_L), (b) vapor pressure deficit (D) and photosynthetic photon flux density (Q). Each data point is a 30 min averaged value and error bars are associated standard error of five sapflux sensors.

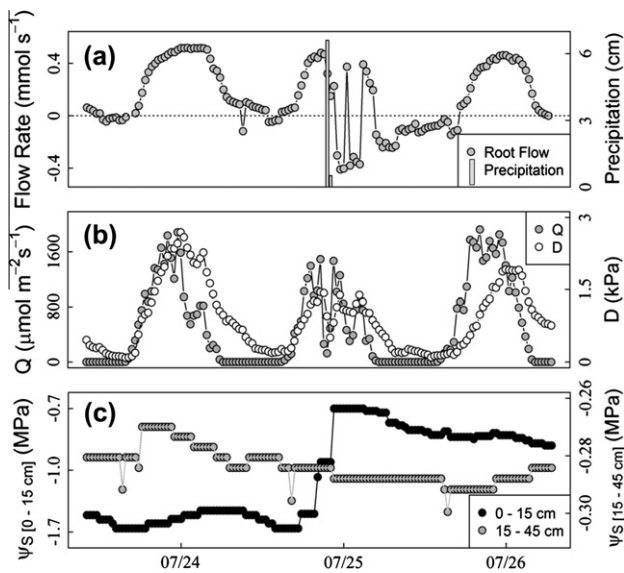


Fig. 3. (a) Diel patterns of root sap flux sensors and precipitation, (b) corresponding photosynthetic photon flux density (Q) and vapor pressure deficit (D), and (c) corresponding soil water potential (Ψ_s) at 0–15 and 15–45 cm depth displaying reverse flow after a rain event. Each data point is a 30 min averaged value.

deeper soil layer (15–45 cm) gradually started wetting (greater Ψ_s at 15–45 cm) a day after rain event (Fig. 3c) at the same time when root sap flux sensor showed negative sap flux (Fig. 3a) and surface soil (0–15 cm) started drying (Fig. 3c).

Both daytime and nighttime USF (half hourly average) increased with increasing atmospheric drought (Fig. 4a) and decreased with increasing soil drought (Fig. 4b). Both stem and root sap flux (30 min average) showed linear increase with increasing Q and displayed a hysteresis effect (30 min lag) in the relationship (Fig. 4c, Table S1 in Supplementary data). The DSF occurred during day and night (Fig. 4d–f) and increased in absolute magnitude with increasing atmospheric drought (Fig. 4d) and declined with increasing soil drought (Fig. 4e). DSF also showed declining relationship with increasing soil moisture deficit between 0–15 cm and 15–45 cm (Fig. 4f) which indicates drying of surface soil.

Due to limited sample size (one root) of root sensors we compared the normalized root data with normalized stem sap flux data to check the representativeness of the data from one root. Comparison of root and stem sap flux sensors showed a linear relationship

($R^2 = 0.52$), with stem sap flux higher than root sap flux at low (0–15%) sap flux values and root sap flux higher than stem sap flux at high (60–80%) sap flux values (Fig. S2 in Supplementary data).

The averaged (five sap flux sensors) daily daytime E_L displayed exponentially saturating response to atmospheric and soil (0–15 cm) drought and combined drought index (Fig. 5a–c and Table S1 in Supporting information). Both soil ($R^2 = 0.61$) and atmospheric ($R^2 = 0.60$) drought displayed equal control on daily daytime transpiration (Fig. 5a and b). Combined drought index explained 72% (Fig. 5c) of variability in the daily daytime transpiration. g_s declined with increasing atmospheric drought (Fig. 5d, $R^2 = 0.54$) and showed a weak declining relationship with soil drought (Fig. 5e) and combined drought index (Fig. 5f). There were several outliers at high g_s under maximum soil drought (Fig. 5e) and most of them were under low temperature (daily average $<18^\circ\text{C}$) and low D (daily average <1.5 kPa) (Fig. 5e). Mean daily nighttime transpiration ($4\text{--}7$ $\text{mmol m}^{-2} \text{s}^{-1}$) varied from 40% to 70% of the maximum daily daytime transpiration (10 $\text{mmol m}^{-2} \text{s}^{-1}$) (Fig. S3 in Supplementary data). Mean daily nighttime D (0.2–1.5 kPa) was 7–50% of the maximum daily daytime D (3 kPa). Soil and atmospheric drought did not show any relationship with nighttime transpiration ($E_{L\text{Night}}$), however, atmospheric drought controlled nighttime stomatal response ($R^2 = 0.78$) (Fig. S3 in Supplementary data).

3.3. Is mountain big sagebrush similar to other arid and semi-arid shrubs and different than mesic trees in terms of reference conductance (g_{SR}) and the ratio ($-m/g_{SR}$)?

Our results indicate that boundary line analysis is robust to binning and $-m/g_{SR}$ did not change with changing bin size (Fig. S5 in Supplementary data). However, sample size showed a significant effect on boundary line analysis. $-m/g_{SR}$ ratio declined with smaller sample size (Fig. S5 in Supplementary data). We conducted boundary line analysis on sample size greater than 100 days to avoid the effect of sample size on the ratio. Sagebrush displayed greater g_{SR} and $-m$ than previously reported values for mesic trees and arid/semi-arid shrubs (Fig. 6a). The average ratio of $-m$ and g_{SR} (Eq. (3) and solid line in Fig. 6a–d) was $0.54 (\pm 0.03)$, which did not differ statistically (P value = 0.109) from the theoretical value (~ 0.6) for mesic trees. The range of ratio between $-m$ and g_{SR} varied from 0.48 to 0.63 among five sap flux sensors (Fig. 6a). The mean ratio between $-m$ and g_{SR} did not differ significantly under varying values of Q (Fig. 6b, P value = 0.503), T_{Air} (Fig. 6c, P value = 0.155), or θ_V (Fig. 6d, P value = 0.756), but data from individual sensors declined with increasing T_{Air} (Fig. 6c) and decreasing θ_V (Fig. 6d) (Table S2 in Supplementary data).

4. Discussion

Our results show that surface soil drought explained higher variability in E_L and g_s than deep soil drought (Table S1 in Supplementary data) which suggests the use of surface soil moisture in ecosystem models for arid and semi-arid shrub ecosystems will not introduce biases by ignoring deep soil moisture. Kwon et al. (2008) used 2004–2005 NEE data for 2 months (June and July) of the growing season from eddy covariance tower, with 2004 being a dry year and 2005 being a wet year. We collected data in the relatively wet year (2005) and the timeframe of our data collection was greater (May–October) than Kwon et al. (June–July), which provided a wide moisture gradient from wet early spring to dry late summer.

Q displayed weak (30 min average) or no relationship (daily daytime data) with g_s (Fig. 4 and Table S1 in Supplementary data), which can be explained by the open canopy and sunny conditions of the study site. Soil and atmospheric drought showed equal

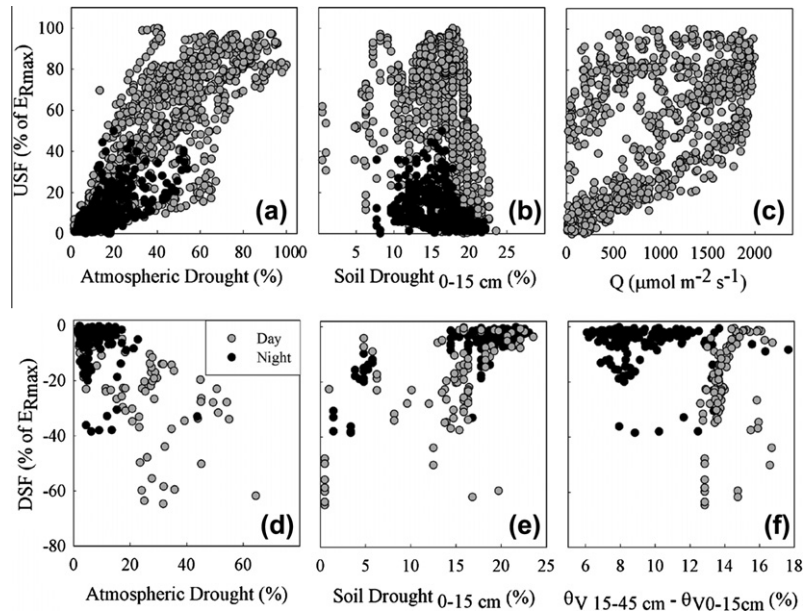


Fig. 4. (a–c) Response of upwards sapflux (USF) to soil (0–15 cm) and atmospheric drought and photosynthetic photon flux density (Q). (d–f) Response of downwards sapflux (DSF) to soil and atmospheric drought and soil moisture deficit between 0–15 cm and 15–45 cm depth. Closed gray symbols are daytime and closed black symbols are nighttime root sapflux standardized by the maximum observed root sapflux during July 9–August 24. Each point is a 30 min averaged value.

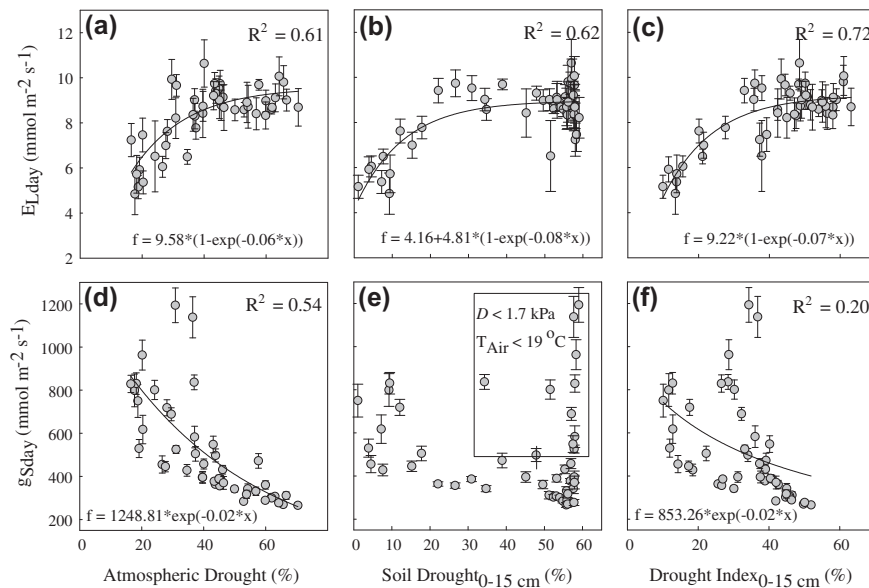


Fig. 5. Response of leaf transpiration (E_L) and leaf stomatal conductance (g_s) to soil (a and d), and atmospheric (b and e) drought and a drought index (c and f). Drought index is an average of soil (0–15 cm) and atmospheric drought. Daily values are calculated from daytime ($Q \geq 10 \mu\text{mol m}^{-2} \text{s}^{-1}$) data.

control (Fig. 5a–c) over E_L , whereas atmospheric drought showed more control over g_s than soil drought (non-significant) (Fig. 5d–f). Previous studies from different ecosystems (Matsumoto et al., 2005 [*Quercus sarrata*]; Irmak and Mutiibwa, 2010 [*Zea mays*]) tested the importance of different meteorological factors in modeling leaf and canopy stomatal conductance and found that Q , T_{Air} and RH contributed the most and θ_v contributed the least. Our field results partially supported these modeling results by showing greater control of atmospheric drought over g_s , which is calculated by T_{Air} and RH , and a weak control of Q over g_s , which could be attributed to different canopy structure as explained above. Despite the different ecosystems (trees and crops versus shrubland), our field data support results reported by Matsumoto et al. (2005) and Irmak and Mutiibwa (2010) showing that soil drought

is a poor predictor for g_s . The relationship between soil drought and g_s becomes weak when soil and atmospheric drought decouple, for instance days when atmospheric drought is low due to low temperature and soil drought is high (Fig. 5e). A previous study on a semi-arid shrub by Ogle and Reynolds (2002) reported an exponential decline in g_s with increasing D and a flat response of $-m$ to D with increasing soil drought, while our data showed a direct effect of soil and atmospheric drought (individually and combined effect) on E_L and g_s . Our results showed similar exponential decline in g_s to D , but we did not see a flat response of stomatal sensitivity to D at lower soil moisture conditions (see below).

Despite the limitations of sample size (one root) and measurement time (3 months) for root sensors, we observed strong signals of upwards (hydraulic lift) and downwards (reverse hydraulic

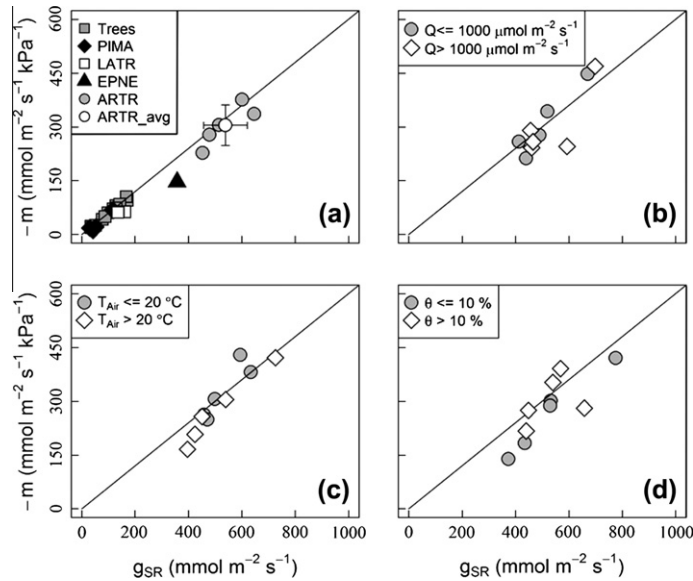


Fig. 6. Relationship between reference stomatal conductance ($g_{SR} = g_S @ 1 \text{ kPa } D$) and sensitivity ($-m$) of g_S to vapor pressure deficit (D). The solid line represents theoretical value of $-m$ versus g_{SR} ratio (~ 0.6) suggesting regulation of minimum leaf water potential (Ψ_{Lmin}) (Oren et al., 1999). (a) Previous data (Oren et al., 1999; Gunderson et al., 2002; Ewers et al., 2001a,b, 2005) for seven mesic tree species (Trees) from the temperate Chequamegon Ecosystem–Atmosphere Study (ChEAS) closely follow 0.6 line despite changes in water status, defoliation and leaf area dynamics. Species with lower m value at a given g_{SR} (Oren et al., 1999 (*Larrea tridentata*, LATR and *Ephedra nevadensis*, EPNE unpublished results), Ogle and Reynolds (2002) (LATR, Ewers et al. (2005) (*Picea mariana*, PIMA)) have less strict Ψ_{Lmin} regulation. This study (*Artemisia tridentata* var. *vaseyana*, ARTR) follows 0.6 line under (b) low ($\leq 10\%$), and high ($> 10\%$) volumetric soil water content ($\theta_{v0-15cm}$), (c) low ($\leq 1000 \mu\text{mol m}^{-2} \text{ s}^{-1}$) and high ($> 1000 \mu\text{mol m}^{-2} \text{ s}^{-1}$) photosynthetic photon flux density (Q) and (d) low ($\leq 20 \text{ }^\circ\text{C}$) and high ($> 20 \text{ }^\circ\text{C}$) air temperature (T_{Air}). Each filled circle for ARTR represents an individual stem sapflux sensor and empty circle represents an average of five stem sapflux sensors with standard error as error bars.

flow) water movement in sagebrush. We use this data as additional evidence to explain the variability in E_L and g_S . Comparison of root and stem sap flux sensors showed a positive linear relationship ($R^2 = 0.52$). At relatively low root sap flux (0–15%), stem sap flux was higher (20–40%) suggesting more use of surface water than deep water and, while at high root sap flux (80–100%), stem sap flux was relatively low (60–80%) (Fig. S2 in Supplementary data). This pattern could be attributed to stomatal regulation during high transpiration rate or leaky roots (Caldwell et al., 1998). Daytime transpiration from root sensors showed a declining relationship with increasing soil drought (Fig. 4b), whereas stem sensors showed an exponentially saturating response (Fig. 5a). These responses indicate an immediate response of root sensors to soil drought and a delayed response of stem sensors, in addition to stomatal regulation of leaf transpiration when water supply from roots started declining.

Nighttime transpiration has been reported across a variety of ecosystem types (5–50% of daytime E_L ; Benyon, 1999; Feild and Holbrook, 2000; Snyder et al., 2003; Bucci et al., 2005; Daley and Phillips, 2006; Cavender-Bares et al., 2007; Dawson et al., 2007; Fisher et al., 2007; Howard and Donovan, 2007; Scholz et al., 2007; Howard et al., 2009) and our results expand the dataset for poorly represented semi-arid shrubs (maximum $E_{Lnight} \sim 70\%$ of the daily maximum E_{Lday}). E_{Lnight} did not show significant relationships with soil and atmospheric drought (Fig. S3 in Supplementary data), which is contrary to prior work by Dawson et al. (2007), showing an increase in nighttime transpiration with increasing soil moisture and D across different ecosystem types. This could be explained by the relationship between D and θ_v in the study area, where under high soil moisture conditions T_{Air} was very low and, as a result, D was always low (Fig. S4 in Supplementary data).

Sagebrush displayed a similar ratio between $-m$ and g_{SR} (Fig. 6a, 0.54 ± 0.03 , Table S2 in Supplementary data) compared to the theoretical value and other mesic trees, which suggests stomatal regulation in sagebrush maintains Ψ_{Lmin} . Our results did not follow previous findings on two other semi-arid shrubs, *Larrea tridentata*

(0.46, Ogle and Reynolds, 2002 (gas exchange data) and 0.31, Pataki, unpublished data cited in Oren et al., 1999) and *Ephedra nevadensis* (0.41, Pataki, unpublished data cited in Oren et al., 1999) (Fig. 6a). A different ratio for sagebrush than other semi-arid shrubs could be due to (1) different range of D (0–4.5 kPa) experienced by sagebrush than reported for *L. tridentata* (Ogle and Reynolds, 2002; 0–10.5 kPa) as the slope of g_S response to D decreases with increased range of D ; and/or (2) use of different technique (gas exchange in Ogle and Reynolds, 2002) which provides substantially smaller number of datapoints than sap flux technique (e.g., this study). Boundary line analysis seems to be sensitive to the number of datapoints included and tended to decrease the ratio when smaller number of datapoints were included (Fig. S5 in Supplementary data). Environmental conditions, such as Q (Fig. 6b), T_{Air} (Fig. 6c), and θ_v (Fig. 6d) did not change the mean ratio but the values for individual sensors increased under low T_{Air} and high θ_v , which is consistent with a previous study by Ewers et al. (2001b).

Loranty et al. (2010) reported a lower g_{SR} for forests with high L and closed canopy, suggesting that competition for light limits the g_{SR} in different stands of mesic forests. Sagebrush (this study) displayed greater g_{SR} and $-m$ than the reported values in literature (Fig. 6a) which can be explained by lower L ($1.2 \text{ m}^2 \text{ m}^{-2}$) and an open canopy ($\sim 39\%$ canopy cover) in our study, resulting in less competition for light. Plants with greater g_{SR} have associated cost of greater absolute reduction in conductance with increasing D than plants with low g_{SR} (Oren et al., 1999). Sagebrush can maintain high g_{SR} for a longer time period as the range of D is not as wide as reported in other semi-arid ecosystems (Ogle and Reynolds, 2002; 0–10.5 kPa) and it has access to deeper soil moisture which is being recharged by its roots during wet conditions (Richards and Caldwell, 1987; this study; Figs. 3 and 4). The combination of high g_{SR} and isohydric regulation increases stomatal sensitivity of sagebrush which is useful for normal, seasonal droughts and allows sagebrush to take advantage of high g_S under low atmospheric drought and high light conditions. Sagebrush

then relies on deep roots for prolonged and more extensive droughts. This may be one reason why mountain big sagebrush is restricted to areas with snowpack. Among all plant functional types, arid/semi-arid shrubs have the highest hydraulic and stomatal conductance per unit leaf area (Mencuccini, 2003). Arid/semi-arid plants have a wide range of evaporative demands (Ogle and Reynolds, 2002: 0–10.5 kPa; present study: 0–4.5 kPa) compared to other vegetation types (e.g., Loranty et al., 2010: 0–2 kPa). As a result of adaptation to their environment, arid/semi-arid shrubs have reduced leaf area which results in several key changes in plant water relations, such as: (1) increased K_L and g_S with reduced leaf area, (2) increased water supply due to less leaf area per unit root area, and (3) increased photosynthesis by open canopy and increased leaf area exposed to incident radiation (Mencuccini, 2003). Additionally, desert shrubs tend to have short canopies (~ 1 m in present study) and plant height is negatively related to K_L (Mencuccini, 2003), which further explains high values of K_L observed in arid/semi-arid shrubs. Moreover, the ability to redistribute soil water (hydraulic redistribution: Caldwell et al., 1987, 1998; present study (Fig. 3)) allows desert shrubs to store the excess water in the deep soil layers during wet conditions and access deep soil water during drought to maintain high K_L , g_{SR} and $-m$ in addition to regulating $\Psi_{Lmin}(-m/g_{SR} \sim 0.6)$. The aforementioned adaptations of arid/semi-arid shrubs make them a potential carbon sink due to increasing CO_2 concentration which will result in increasing assimilation and decreasing g_S (stomatal optimization theory – Katul et al., 2009).

Our work has demonstrated that hydraulic mechanisms operating in semi-arid sagebrush ecosystems, such as nighttime transpiration and reverse hydraulic flow help sagebrush to regulate g_S and $\Psi_{Lmin}(-m/g_{SR} \sim 0.6)$, despite the costs of higher g_{SR} and $-m$. This study tested a plant-hydraulic-model and showed that sagebrush has a suite of water relation adaptations, which should be considered when modeling ecosystem water loss.

4.1. Implications for ecosystem and hydrologic modeling

Isohyric behavior of sagebrush indicates that well-known forest ecosystem and hydrology models can be used for modeling water, energy and carbon cycles from sagebrush and similar ecosystems. A simple modification (e.g., higher g_{SR} , $-m$) and incorporation of hydraulic redistribution in ecosystem and hydrology models which were designed originally for forest ecosystems (e.g., TREES (Mackay et al., 2003)) may improve future prediction of water, energy and carbon cycles of these widely distributed sagebrush ecosystems and other similar arid and semi-arid shrublands.

Acknowledgements

This study was supported by the National Research Initiative of the USDA Cooperative State Research, Education and Extension Service, Grant (# 2003-35101-13652). Partial funding was also provided by the National Science Foundation (# EPS-0447681) and the Agricultural Experiment Station Competitive Grants Program, Project (# WYO-401-06). We are thankful to Dr. M.B. Cleary and Sarah Adelman for their help in data collection. We are grateful to Dr. David Williams, Landscape Ecology group at Penn State and anonymous reviewers for their feedback on earlier draft of this manuscript.

Appendix A. Supplementary material

Supplementary data associated with this article can be found, in the online version, at <http://dx.doi.org/10.1016/j.jhydrol.2012.07.008>.

References

- Abramoff, M.D., Magelhaes, P.J., Ram, S.J., 2004. Image processing with ImageJ. *Biophoton. Int.* 11, 36–42.
- Addington, R.N., Mitchell, R.J., Oren, R., Donovan, L.A., 2004. Stomatal sensitivity to vapor pressure deficit and its relationship to hydraulic conductance in *Pinus palustris*. *Tree Physiol.* 24, 561–569.
- Baldocchi, D.D., 2005. The role of biodiversity on the evaporation of forests. In: Scherer-Lorenzen, M., Körner, C., Schulze, E.-D. (Eds.), *Forest Diversity and Function Ecological Studies*. Springer, Berlin, Heidelberg, pp. 131–148.
- Baldocchi, D.D., Wilson, K.B., Gu, L., 2002. How the environment, canopy structure and canopy physiological functioning influence carbon, water and energy fluxes of a temperate broad-leaved deciduous forest – an assessment with the biophysical model CANOAK. *Tree Physiol.* 22, 1065–1077.
- Ball, J.T., Woodrow, I.E., Berry, J.A., 1987. A model predicting stomatal conductance and its contribution to the control of photosynthesis under different environmental conditions. *Prog. Photosyn. Res.* 4, 221–224.
- Bates, B.C., Kundzewicz, Z.W., Wu, S., Palutikof, J.P., 2008. *Climate Change and Water*. Technical Paper of the Intergovernmental Panel on Climate Change (Technical Paper of the Intergovernmental Panel on Climate Change No. IV). IPCC Secretariat, Geneva.
- Benyon, R.G., 1999. Nighttime water use in an irrigated *Eucalyptus grandis* plantation. *Tree Physiol.* 19, 853–859.
- Brooks, J.R., Meinzer, F.C., Warren, J.M., Domec, J.-C., Coulombe, R., 2006. Hydraulic redistribution in a Douglas-fir forest: lessons from system manipulations. *Plant Cell Environ.* 29, 138–150.
- Bucci, S.J., Goldstein, G., Meinzer, F.C., Franco, A.C., Campanello, P., Scholz, F.G., 2005. Mechanisms contributing to seasonal homeostasis of minimum leaf water potential and predawn disequilibrium between soil and plant water potential in Neotropical savanna trees. *Trees (Berl. West)* 19, 296–304.
- Caldwell, M.M., Richards, J.H., 1989. Hydraulic lift: water efflux from upper roots improves effectiveness of water uptake by deep roots. *Oecologia* 79, 1–5.
- Caldwell, M.M., Richards, J.H., Manwaring, J.H., Eissenstat, D.M., 1987. Rapid shifts in phosphate acquisition show direct competition between neighbouring plants. *Nature* 327, 615–616.
- Caldwell, M.M., Dawson, T.E., Richards, J.H., 1998. Hydraulic lift: consequences of water efflux from the roots of plants. *Oecologia* 113, 151–161.
- Cavender-Bares, J., Sack, L., Savage, J., 2007. Atmospheric and soil drought reduce nocturnal conductance in live oaks. *Tree Physiol.* 27, 611–620.
- Cermák, J., Cienciala, E., Kucera, J., Lindroth, A., Bednářová, E., 1995. Individual variation of sap-flow rate in large pine and spruce trees and stand transpiration: a pilot study at the central NOPEX site. *J. Hydrol.* 168, 17–27.
- Čermák, J., Deml, M., Penka, M., 1973. A new method of sap flow rate determination in trees. *Biol. Plant.* 15, 171–178.
- Chambers, J.L., Hinckley, T.M., Cox, G.S., Metcalf, C.L., Aslin, R.G., 1985. Boundary-line analysis and models of leaf conductance for four oak-hickory forest species. *Foren. Sci.* 31, 437–450.
- Cienciala, E., Eckersten, H., Lindroth, A., Hällgren, J.-E., 1994. Simulated and measured water uptake by *Picea abies* under non-limiting soil water conditions. *Agric. For. Meteorol.* 71, 147–164.
- Cleary, M.B., Pendall, E., Ewers, B.E., 2010. Aboveground and belowground carbon pools after fire in mountain big sagebrush steppe. *Rangel. Ecol. Manage.* 63, 187–196.
- Cochard, H., Bréda, N., Granier, A., 1996. Whole tree hydraulic conductance and water loss regulation in *Quercus* during drought: evidence for stomatal control of embolism? *Ann. Sci. Forest.* 53, 197–206.
- Cowan, I.R., Farquhar, G.D., 1977. Stomatal function in relation to leaf metabolism and environment. *Symp. Soc. Exp. Biol.* 31, 471–505.
- Daley, M.J., Phillips, N.G., 2006. Interspecific variation in nighttime transpiration and stomatal conductance in a mixed New England deciduous forest. *Tree Physiol.* 26, 411–419.
- Dawson, T.E., Burgess, S.S.O., Tu, K.P., Oliveira, R.S., Santiago, L.S., Fisher, J.B., Simonin, K.A., Ambrose, A.R., 2007. Nighttime transpiration in woody plants from contrasting ecosystems. *Tree Physiol.* 27, 561–575.
- Easterling, D.R., Meehl, G.A., Parmesan, C., Changnon, S.A., Karl, T.R., Mearns, L.O., 2006. Climate extremes: observations, modeling, and impacts. *Science* 289, 2068–2074.
- Ewers, B.E., Mackay, D.S., Gower, S.T., Ahl, D.E., Samanta, S.N.B., 2002. Tree species effects on stand transpiration in northern Wisconsin. *Water Resour. Res.* 38, 1–11.
- Ewers, B.E., Mackay, D.S., Samanta, S., 2007. Interannual consistency in canopy stomatal conductance control of leaf water potential across seven tree species. *Tree Physiol.* 27, 11–24.
- Ewers, B., Pendall, E., 2008. Spatial patterns in leaf area and plant functional type cover across chronosequences of sagebrush ecosystems. *Plant Ecol.* 194, 67–83.
- Ewers, B.E., Oren, R., Johnsen, K.H., Landsberg, J.J., 2001a. Estimating maximum mean canopy stomatal conductance for use in models. *Can. J. For. Res.* 31, 198–207.
- Ewers, B.E., Oren, R., 2000. Analyses of assumptions and errors in the calculation of stomatal conductance from sap flux measurements. *Tree Physiol.* 20, 579–589.
- Ewers, B.E., Oren, R., Phillips, N., Stromgren, M., Linder, S., 2001b. Mean canopy stomatal conductance responses to water and nutrient availabilities in *Picea abies* and *Pinus taeda*. *Tree Physiol.* 21, 841–850.

- Ewers, B.E., Gower, S.T., Bond-Lamberty, B., Wang, C.K., 2005. Effects of stand age and tree species on canopy transpiration and average stomatal conductance of boreal forests. *Plant. Cell. Environ.* 28, 660–678.
- Feild, T.S., Holbrook, N.M., 2000. Xylem sap flow and stem hydraulics of the vesselless angiosperm *Drimys granadensis* (Winteraceae) in a Costa Rican elfin forest. *Plant Cell Environ.* 23, 1067–1077.
- Fisher, R.A., Williams, M., daCosta, A., Malhi, Y., daCOSTA, R.F., Almeida, S., Meir, P., 2007. The response of an Eastern Amazonian rain forest to drought stress: results and modelling analyses from a throughfall exclusion experiment. *Global Change Biol.* 13, 2361–2378.
- Franks, P.J., Drake, P.L., Froend, R.H., 2007. Anisohydric but isohydrodynamic: seasonally constant plant water potential gradient explained by a stomatal control mechanism incorporating variable plant hydraulic conductance. *Plant Cell Environ.* 30, 19–30.
- Franks, P.J., 2004. Stomatal control and hydraulic conductance, with special reference to tall trees. *Tree Physiol.* 24, 865–878.
- Fujii, H., Chinnusamy, V., Rodrigues, A., Rubio, S., Antoni, R., Park, S.-Y., Cutler, S.R., Sheen, J., Rodriguez, P.L., Zhu, J.-K., 2009. In vitro reconstitution of an abscisic acid signalling pathway. *Nature* 462, 660–664.
- Goff, J.A., Gratch, S., 1946. Low-pressure properties of water from –160 to 212 F. *Trans. Heat Pip. Air Cond.* 52, 95–122.
- Gunderson, C.A., Sholtis, J.D., Wullschlegel, S.D., Tissue, D.T., Hanson, P.J., Norby, R.J., 2002. Environmental and stomatal control of photosynthetic enhancement in the canopy of a sweetgum (*Liquidambar styraciflua* L.) plantation during 3 years of CO₂ enrichment. *Plant Cell Environ.* 25, 379–393.
- Howard, A.R., Donovan, L.A., 2007. Helianthus nighttime conductance and transpiration respond to soil water but not nutrient availability. *Plant Physiol.* 143, 145–155.
- Howard, A.R., van Iersel, M.W., Richards, J.H., Donovan, L.A., 2009. Night-time transpiration can decrease hydraulic redistribution. *Plant Cell Environ.* 32, 1060–1070.
- Hultine, K.R., Williams, D.G., Burgess, S.S.O., Keefer, T.O., 2003. Contrasting patterns of hydraulic redistribution in three desert phreatophytes. *Oecologia* 135, 167–175.
- Irmak, S., Mutiibwa, D., 2010. On the dynamics of canopy resistance: Generalized linear estimation and relationships with primary micrometeorological variables. *Water Resour. Res.* 46, W08526.
- Jarvis, P.G., 1976. The interpretation of the variations in leaf water potential and stomatal conductance found in canopies in the field. *Philos. Trans. Roy. Soc. Lond. Ser. B: Biol. Sci.* 273, 593–610.
- Jarvis, P.G., 1995. Scaling processes and problems. *Plant Cell Environ.* 18, 1079–1089.
- Johnson, D.M., Woodruff, D.R., McCulloh, K.A., Meinzer, F.C., 2009. Leaf hydraulic conductance, measured in situ, declines and recovers daily: leaf hydraulics, water potential and stomatal conductance in four temperate and three tropical tree species. *Tree Physiol.* 29, 879–887.
- Katul, G.G., Palmroth, S., Oren, R., 2009. Leaf stomatal responses to vapour pressure deficit under current and CO₂-enriched atmosphere explained by the economics of gas exchange. *Plant Cell Environ.* 32, 968–979.
- Katul, G.G., Leuning, R., Oren, R., 2003. Relationship between plant hydraulic and biochemical properties derived from a steady-state coupled water and carbon transport model. *Plant Cell Environ.* 26, 339–350.
- Körner, C., 1994. Leaf diffusive conductances in the major vegetation types of the globe. In: Schulze, E.-D., Caldwell, M.M. (Eds.), *Ecophysiology of Photosynthesis Ecological Studies*. Springer-Verlag, Berlin, pp. 463–485.
- Köstner, B.M.M., Schulze, E.-D., Kelliher, F.M., Hollinger, D.Y., Byers, J.N., Hunt, J.E., McSeveny, T.M., Meserth, R., Weir, P.L., 1992. Transpiration and canopy conductance in a pristine broad-leaved forest of nothofagus: an analysis of xylem sap flow and eddy correlation measurements. *Oecologia* 91, 350–359.
- Köstner, B., Granier, A., Cermák, J., 1998. Sapflow measurements in forest stands: methods and uncertainties. *Ann. For. Sci.* 55, 13–27.
- Kučera, J., 1977. A system for water flux measurements in plants.
- Kučera, J., Cermák, J., Penka, M., 1977. Improved thermal method of continual recording the transpiration flow rate dynamics. *Biol. Plant.* 19, 413–420.
- Kwon, H., Pendall, E., Ewers, B.E., Cleary, M., Naithani, K., 2008. Spring drought regulates summer net ecosystem CO₂ exchange in a sagebrush-steppe ecosystem. *Agric. For. Meteorol.* 148, 381–391.
- Lai, C.-T., Katul, G., Butnor, J., Siqueira, M., Ellsworth, D., Maier, C., Johnsen, K., Mckeand, S., Oren, R., 2002. Modelling the limits on the response of net carbon exchange to fertilization in a south-eastern pine forest. *Plant Cell Environ.* 25, 1095–1120.
- Lei, H., Zhi-Shan, Z., Xin-Rong, L., 2010. Sap flow of *Artemisia ordosica* and the influence of environmental factors in a revegetated desert area: Tengger Desert, China. *Hydrol. Process.* 24, 1248–1253.
- Loranty, M.M., Mackay, D.S., Ewers, B.E., Traver, E., Kruger, E.L., 2010. Contribution of competition for light to within-species variability in stomatal conductance. *Water Resour. Res.* 46, 18.
- Mackay, D.S., Ahl, D.E., Ewers, B.E., Samanta, S., Gower, S.T., Burrows, S.N., 2003. Physiological tradeoffs in the parameterization of a model of canopy transpiration. *Adv. Water Resour.* 26, 179–194.
- Mackay, D.S., Ewers, B.E., Loranty, M.M., Kruger, E.L., 2010. On the representativeness of plot size and location for scaling transpiration from trees to a stand. *J. Geophys. Res.* 115, 14.
- Martin, T.A., Brown, K.J., Cermák, J., Ceulemans, R., Kučera, J., Meinzer, F.C., Rombold, J.S., Sprugel, D.G., Hinckley, T.M., 1997. Crown conductance and tree and stand transpiration in a second-growth *Abies amabilis* forest. *Can. J. For. Res.* 27, 797–808.
- Matsumoto, K., Ohta, T., Tanaka, T., 2005. Dependence of stomatal conductance on leaf chlorophyll concentration and meteorological variables. *Agric. For. Meteorol.* 132, 44–57.
- Meinzer, F.C., Grantz, D.A., 1991. Coordination of stomatal, hydraulic, and canopy boundary layer properties: do stomata balance conductances by measuring transpiration? *Physiol. Plant.* 83, 324–329.
- Mencuccini, M., 2003. The ecological significance of long-distance water transport: short-term regulation, long-term acclimation and the hydraulic costs of stature across plant life forms. *Plant Cell Environ.* 26, 163–182.
- Monteith, J.L., 1995. A reinterpretation of stomatal responses to humidity. *Plant Cell Environ.* 18, 357–364.
- Monteith, J., Unsworth, M., 1990. *Principles of Environmental Physics*, second ed. Edward Arnold, London.
- Mott, K.A., Franks, P.J., 2001. The role of epidermal turgor in stomatal interactions following a local perturbation in humidity. *Plant Cell Environ.* 24, 657–662.
- Mott, K.A., Parkhurst, D.F., 1991. Stomatal responses to humidity in air and helox. *Plant Cell Environ.* 14, 509–515.
- Nardini, A., Salleo, S., 2000. Limitation of stomatal conductance by hydraulic traits: sensing or preventing xylem cavitation? *Trees* 15, 14–24.
- NAST, 2001. *Climate Change Impacts on the United States: Potential Consequences of Climate Variability and Change (Foundation Report)*, (National Assessment Synthesis Team) Report for the US Global Change Research Program. Cambridge University Press, Cambridge, UK.
- Ogle, K., Reynolds, J.F., 2002. Desert dogma revisited: coupling of stomatal conductance and photosynthesis in the desert shrub *Larrea tridentata*. *Plant Cell Environ.* 25, 909–921.
- Ogle, K., Reynolds, J.F., 2004. Plant responses to precipitation in desert ecosystems: integrating functional types, pulses, thresholds, and delays. *Oecologia* 141, 282–294.
- Oren, R., Sperry, J.S., Ewers, B.E., Pataki, D.E., Phillips, N., Megonigal, J.P., 2001. Sensitivity of mean canopy stomatal conductance to vapor pressure deficit in a flooded *Taxodium distichum* L. forest: hydraulic and non-hydraulic effects. *Oecologia* 126, 21–29.
- Oren, R., Sperry, J.S., Katul, G.G., Pataki, D.E., Ewers, B.E., Phillips, N., Schäfer, K.V.R., 1999. Survey and synthesis of intra- and interspecific variation in stomatal sensitivity to vapour pressure deficit. *Plant Cell Environ.* 22, 1515–1526.
- Pandey, S., Wang, R.-S., Wilson, L., Li, S., Zhao, Z., Gookin, T.E., Assmann, S.M., Albert, R., 2010. Boolean modeling of transcriptome data reveals novel modes of heterotrimeric G-protein action. *Mol. Syst. Biol.* 6.
- Pataki, D.E., Huxman, T.E., Jordan, D.N., Zitzer, S.F., Coleman, J.S., Smith, S.D., Nowak, R.S., Seemann, J.R., 2000. Water use of two Mojave Desert shrubs under elevated CO₂. *Global Change Biol.* 6, 889–897.
- Pearcy, R.W., Ehleringer, J.R., Mooney, H.A., Rundel, P.W. (Eds.), 1989. *Plant Physiological Ecology. Field Methods and Instrumentation*, first ed. Chapman and Hall, New York.
- Pezeshki, S.R., Hinckley, T.M., 1988. Water relations characteristics of *Alnus rubra* and *Populus trichocarpa*: responses to field drought. *Can. J. For. Res.* 18, 1159–1166.
- Phillips, N., Oren, R., 1998. A comparison of daily representations of canopy conductance based on two conditional time-averaging methods and the dependence of daily conductance on environmental factors. *Ann. For. Sci.* 55, 217–235.
- Qu, Y., Kang, S., Li, F., Zhang, J., Xia, G., Li, W., 2007. Xylem sap flows of irrigated *Tamarix elongata* Ledeb and the influence of environmental factors in the desert region of Northwest China. *Hydrol. Process.* 21, 1363–1369.
- R Development Core Team, 2010. *R: A Language and Environment for Statistical Computing*. R Foundation for Statistical Computing, Vienna, Austria.
- Reynolds, J.F., 2000. Desertification. In: Levin, S.A. (Ed.), *Encyclopedia of Biodiversity*. Academic Press, San Diego, pp. 61–78.
- Richards, J.H., Caldwell, M.M., 1987. Hydraulic lift: Substantial nocturnal water transport between soil layers by *Artemisia tridentata* roots. *Oecologia* 73, 486–489.
- Saliendra, N.Z., Sperry, J.S., Comstock, J.P., 1995. Influence of leaf water status on stomatal response to humidity, hydraulic conductance, and soil drought in *Betula occidentalis*. *Planta* 196, 357–366.
- Salleo, S., Nardini, A., Pitt, F., Gullo, M.A.L., 2000. Xylem cavitation and hydraulic control of stomatal conductance in Laurel (*Laurus nobilis* L.). *Plant Cell Environ.* 23, 71–79.
- Schäfer, K.V.R., Oren, R., Tenhunen, J.D., 2000. The effect of tree height on crown level stomatal conductance. *Plant Cell Environ.* 23, 365–375.
- Schäfer, K.V.R., Oren, R., Ellsworth, D.S., Lai, C.-T., Herrick, J.D., Finzi, A.C., Richter, D.D., Katul, G.G., 2003. Exposure to an enriched CO₂ atmosphere alters carbon assimilation and allocation in a pine forest ecosystem. *Global Change Biol.* 9, 1378–1400.
- Schlesinger, W.H., 1997. *Biogeochemistry: An Analysis of Global Change*, second ed. Academic Press, UK.
- Scholz, F.G., Bucci, S.J., Goldstein, G., Meinzer, F.C., Franco, A.C., Miralles-Wilhelm, F., 2007. Removal of nutrient limitations by long-term fertilization decreases nocturnal water loss in savanna trees. *Tree Physiol.* 27, 551–559.
- Sellers, P.J., Dickinson, R.E., Randall, D.A., Betts, A.K., Hall, F.G., Berry, J.A., Collatz, G.J., Denning, A.S., Mooney, H.A., Nobre, C.A., Sato, N., Field, C.B., Henderson-Sellers, A., 1997. Modeling the exchanges of energy, water, and carbon between continents and the atmosphere. *Science* 275, 502–509.

- Sivakumar, M., Das, H., Brunini, O., 2005. Impacts of present and future climate variability and change on agriculture and forestry in the arid and semi-arid tropics. *Clim. Change* 70, 31–72.
- Smith, D.M., Allen, S.J., 1996. Measurement of sap flow in plant stems. *J. Exp. Bot.* 47, 1833–1844.
- Snyder, K.A., Richards, J.H., Donovan, L.A., 2003. Night-time conductance in C₃ and C₄ species: do plants lose water at night? *J. Exp. Bot.* 54, 861–865.
- Sokal, R.R., Rohlf, F.J., 1995. *Biometry*, third ed. Macmillan.
- Sperry, J.S., 1995. Limitations on stem water transport and their consequences. In: Gartner, B.L. (Ed.), *Plant Stems: Physiology and Functional Morphology*, Physiological Ecology. Elsevier, Academic Press, Inc., San Diego, pp. 105–224.
- Sperry, J.S., Adler, F.R., Campbell, G.S., Comstock, J.P., 1998. Limitation of plant water use by rhizosphere and xylem conductance: results from a model. *Plant Cell Environ.* 21, 347–359.
- Sturges, D.L., 1977. Soil water withdrawal and root characteristics of big sagebrush. *Am. Midl. Nat.* 98, 257–274.
- Tardieu, F., Simonneau, T., 1998. Variability among species of stomatal control under fluctuating soil water status and evaporative demand: modelling isohydric and anisohydric behaviours. *J. Exp. Bot.* 49, 419–432.
- Tyree, M.T., Sperry, J.S., 1989. Vulnerability of xylem to cavitation and embolism. *Annu. Rev. Plant. Physiol. Plant. Mol. Biol.* 40, 19–36.
- West, N.E., 1983. Western Intermountain sagebrush steppe. In: West, N.E. (Ed.), *Ecosystems of the World*. Elsevier, New York, USA, pp. 351–374.
- Whitehead, D., Edwards, W.R.N., Jarvis, P.G., 1984. Conducting sapwood area, foliage area, and permeability in mature trees of *Picea sitchensis* and *Pinus contorta*. *Can. J. For. Res.* 14, 940–947.
- Whitehead, D., Jarvis, P.G., 1981. Coniferous forests and plantations. In: Kozlowski, T.T. (Ed.), *Water Deficits and Plant Growth*. Academic Press, UK, pp. 49–152.